Emergent topology under slow non-adiabatic quantum dynamics

Junchen Ye
&
Fuxiang Li, Prof.

School of Physics and Electronics, Hunan University

湖南大學
HUNAN UNIVERSITY

Changsha 410082, China
July 26, 2020

CONTENT

Background

Is there still a non-adiabatic dynamical characterization?

What Happened?

Excitations?

Topological Defects?

Is it detrimental?

* D. Guery-Odelin, etc. Rev. Mod. Phys. 91, 045001 (2019).

* Zhang L, etc. Sci. Bull. 63, 1385 (2018).

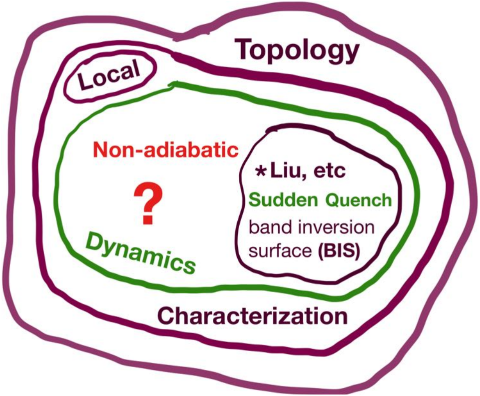

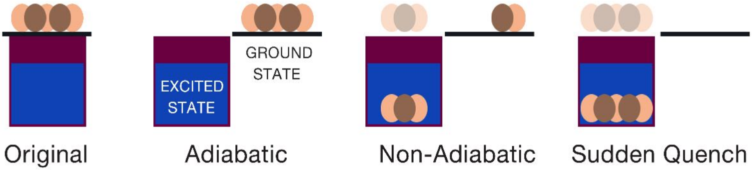

Generalized Landau-Zener problem

Coulomb Like Time-Dependent Hamiltonian

Coulomb Like Time-Dependent Hamiltonian

$$H(t) = \boldsymbol{\sigma}\cdot\mathbf{h}(t)$$

$$= \begin{pmatrix} g/t + \varepsilon\cos\theta & \varepsilon\sin\theta e^{-i\varphi} \\ \varepsilon\sin\theta e^{i\varphi} & -(g/t+\varepsilon\cos\theta) \end{pmatrix}$$

The evolution of state vector $|\psi(t)\rangle$ is governed by $i\hbar\frac{d}{dt}|\psi(t)\rangle = H(t)|\psi(t)\rangle$.

Two Instantaneous Eigenstates

$$(1,0)^T \rightarrow |+\rangle = (\cos\frac{\theta}{2}e^{-i\varphi}, \sin\frac{\theta}{2})^T;$$

$$(0,1)^T \rightarrow |-\rangle = (\sin\frac{\theta}{2}e^{-i\varphi}, -\cos\frac{\theta}{2})^T;$$

Transition Probability $|\downarrow\rangle \rightarrow |+\rangle$

$$P = \frac{e^{-2\pi g\cos\theta} - e^{-2\pi g}}{e^{2\pi g} - e^{-2\pi g}}$$

which is independent of parameters ε and φ.

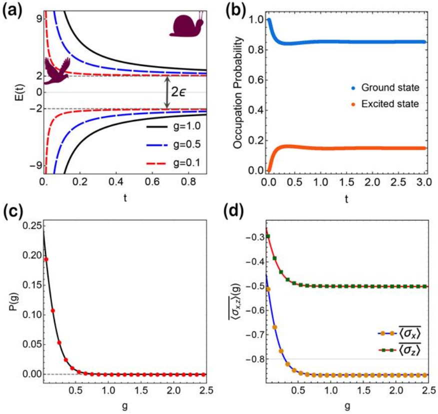

Figure 1: Instantaneous eigen-energies as functions of time t for different quench time g. Other parameters: $\varepsilon = 2$, $\varphi = 0$, and $\theta = \pi/3$, and the same for (b-d). (b) The occupation probability of time-dependent state vector $|\psi(t)\rangle$ on the two instantaneous eigenstates, with $g = 0.1$. (c)Transition probability P from initial ground state to final excited state as a function of g. (d) Time-averaged spin polarizations as functions of varying g.

Generalized Landau-Zener problem

Related Spin Dynamics

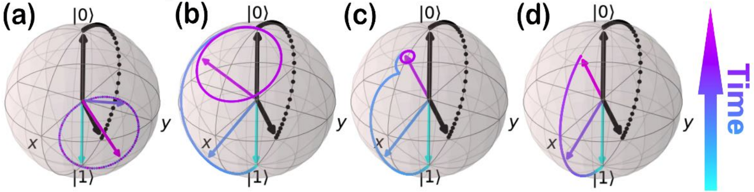

Figure 2: Illustration of the crossover from sudden quench regime to adiabatic regime by four Bloch spheres expressing the dynamics of spin vector. Spin polarization $\boldsymbol{\sigma}(t)$ (colored arrow) and the unit vector of the time-dependent effective field $\boldsymbol{n}(t)$ (black arrow) are shown with evolving time. (a) Sudden quench is approximated with $g = 0.025$; (b) and (c) Non-adiabatic dynamics with different quench time, $g = 5$ (b) and $g = 10$ (c). (d)Adiabatic limit plotted with $g = 100$.

$$H(t) = \boldsymbol{\sigma} \cdot \mathbf{h}(t);$$

$$h_z = \frac{g}{t} + \cos\theta, \;\; h_x = \sin\theta\cos\varphi, \;\; h_y = \sin\theta\sin\varphi.$$

following Bloch equation derived from the Heisenberg equation of motion:

$$\frac{d}{dt}\boldsymbol{\sigma}(t) = 2\mathbf{h}(t) \times \boldsymbol{\sigma}(t).$$

we get the time averaged spin polarization in three regimes:

$$\overline{\langle\boldsymbol{\sigma}\rangle}_{sq} = -\mathbf{n}\cos\theta; \quad \overline{\langle\boldsymbol{\sigma}\rangle} = (2P-1)\mathbf{n}; \quad \overline{\langle\boldsymbol{\sigma}\rangle}_{ad} = -\mathbf{n};$$

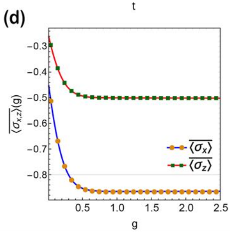

Slow Quench Hamiltonian

1D Case of Topological Quantum Phases

Generical Hamiltanion

$$\mathcal{H}(\mathbf{k}) = \mathbf{h}(\mathbf{k}) \cdot \boldsymbol{\gamma} = \sum_{i=0}^{d} h_i(\mathbf{k})\gamma_i;$$
$$h_0(\mathbf{k}) = 0; \quad (BIS)$$
$$\nu(h_0, \mathbf{h}_{so}) \Leftrightarrow \omega_{d-1}(\mathbf{h}_{so}), \; (Bulk - Surface$$
$$dD \Leftrightarrow (d-1)D; \quad Correspondence)$$

Sudden Quench

$$On\ BISs,\ h_0 \gg |\mathbf{h}_{so}(\mathbf{k})| \to 0,$$
$$\Rightarrow \cos\theta(\mathbf{k}) = 0;$$
$$\Rightarrow \overline{\langle \boldsymbol{\sigma} \rangle}_{sq} = -\mathbf{n}\cos\theta = 0;$$

Non-adiabatic dynamics

$$h_x = t_{so} \sin k_x = h_{so},$$
$$h_z(t) = \frac{g}{t} + m_z - t_0 \cos k_x = h_0(t);$$

$$On\ BISs,\ h_0 \gg |\mathbf{h}_{so}(k_x)| \to 0,$$
$$BUT\ !\ (2P(k_x) - 1) \neq 0,$$
$$Only\ !\ \overline{\langle \boldsymbol{\sigma} \rangle}_0 = (2P - 1)n_0 = 0;$$

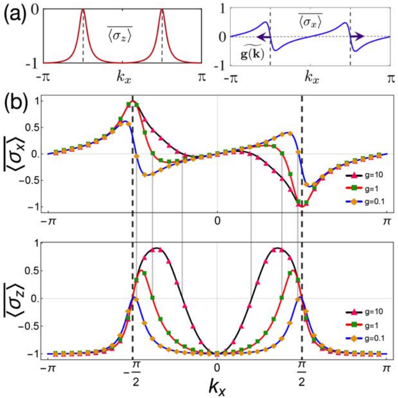

Figure 3: (a) 1D Case of Sudden quench in Liu's Paper (Sci.Bull.2018). (b) $\overline{\langle \boldsymbol{\sigma} \rangle}$ of 1D topological model after Slow quench dynamics. with $t_{so} = 0.2t_0$ and $m_z = 0$. Here we set $t_0 = 1$. Two different kinds of zeros appear in the the z component, which are highlighted by vertical dashed lines (BIS) and gray lines (SIS, new), respectively. The topological spin texture can be determined by the values of x-component on the BIS. In this case, $\overline{\langle \sigma_x \rangle}$ has opposite signs on the two BIS points, and thus gives the winding number $+1$.

Slow Quench Hamiltonian

2D Case of Topological Quantum Phases

Slow Quench Hamiltonian along h_z

$$\begin{aligned}
\mathcal{H}(\mathbf{k}) &= \mathbf{h}(\mathbf{k}, t) \cdot \boldsymbol{\sigma}; \\
h_x &= m_x + t_{so}^x \sin k_x, \\
h_y &= m_y + t_{so}^y \sin k_y, \\
h_z &= \frac{g}{t} + m_z - t_0 \cos k_x - t_0 \cos k_y;
\end{aligned}$$

Topological property of post-quench Hamiltonian:

For $0 < m_z < 2t_0 \Rightarrow C_1 = -1$,
While for $-2t_0 < m_z < 0 \Rightarrow C_1 = +1$.

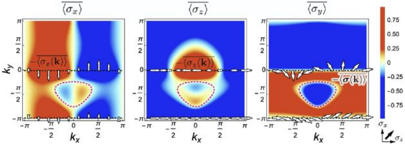

Figure 4: Slow quench along $h_y(\boldsymbol{k})$ axis. numerical results, with $m_z = t_0$, $m_x = 0$, $t_{so}^x = 0.5t_{so}^y = t_0$, and we set $t_0 = 1$ and $g = 1$. There are two BISs (black dash line). While the winding of $-\overline{\boldsymbol{\sigma}}$ (white arrow) is trivial along $k_y = -\pi$, the non-zero winding number along $k_y = 0$ indicates the topological phase with Chern number $C_1 = -1$.

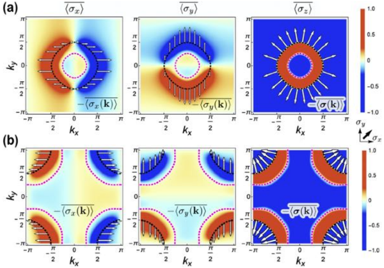

Figure 5: Analytical results for 2D Chern insulators in different post-quench regime with $m_x = m_y = 0$, $t_{so}^{x,y} = 0.2t_0$. Here we set $t_0 = 1$ and $g = 5$. (a). $\overline{\langle \boldsymbol{\sigma} \rangle}$ are plotted with $m_z = t_0$. pink dashed ring is SIS, black dashed ring is BIS. The white arrows are the vectors formed by $-\overline{\langle \boldsymbol{\sigma} \rangle}$, indicating a nontrivial topological spin texture with Chern number $C_1 = -1$. (b). Same case with $m_z = -t_0$. As the winding of white arrows on BIS is opposite to that in (a), we identify the topological phase with the Chern number $C_1 = 1$.

Slow Quench Hamiltonian along h_y

$$h_y(t) = g/t + m_y + t_{so}^y \sin k_y;$$

Quenching under Linear Quench Protocol

1D Case of Linear slow quench

1D Linear Slow Quench Hamiltonian

$$\mathcal{H}(\mathbf{k}) = \mathbf{h}(\mathbf{k}, t) \cdot \boldsymbol{\sigma};$$
$$h_x = t_{so} \sin k_x = h_{so},$$
$$h_z(t) = \beta t + m_z - t_0 \cos k_x = h_0(t);$$

Here, β describes how fast the quench is. The quench starts from $t = -\infty$ to a finite value of t.

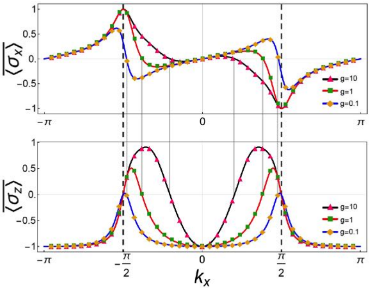

Figure 6: Analytical results for the 1D topological model with Coulomb-like quench protocol g/t.

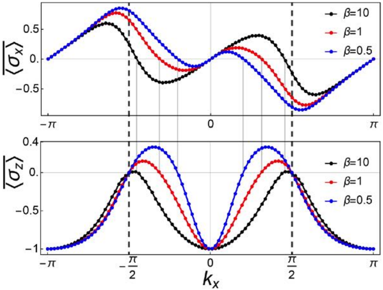

Figure 7: Numerical results for the 1D topological model with linear quench protocol βt.

Time-averaged components $\overline{\langle \sigma_x \rangle}$ (upper panel) and $\overline{\langle \sigma_z \rangle}$ (lower panel) of spin texture $\overline{\langle \boldsymbol{\sigma} \rangle}$ are shown for different values of quench speed β. The quench is taken from $t = -20$ to $t = 0$ with $m_z = 0$ and $t_{so} = 0.6t_0$ so that the post-quench Hamiltonian is in topologically nontrivial phase. After the quench, the system is under free evolution and the spin polarization is averaged over a long time period. The SISs and BISs are denoted by gray lines and dashed lines, respectively. The opposite sign of $-\overline{\langle \boldsymbol{\sigma}_x \rangle}$ on BIS characterizes the nontrivial topology, and gives the winding number $+1$.

Quenching under Linear Quench Protocol

2D Case of Linear slow quench

2D Linear Slow Quench Hamiltonian

$$\mathcal{H}(\mathbf{k}) = \mathbf{h}(\mathbf{k}, t) \cdot \boldsymbol{\sigma};$$
$$h_x = m_x + t_{so}^x \sin k_x;$$
$$h_y = m_y + t_{so}^y \sin k_y;$$
$$h_z = \beta t + m_z - t_0 \cos k_x - t_0 \cos k_y;$$

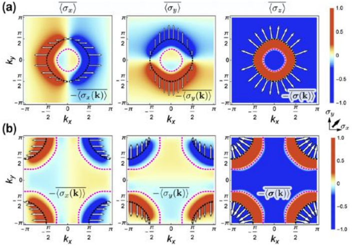

Figure 8: Analytical results for the 2D topological model with Coulomb-like quench protocol g/t.

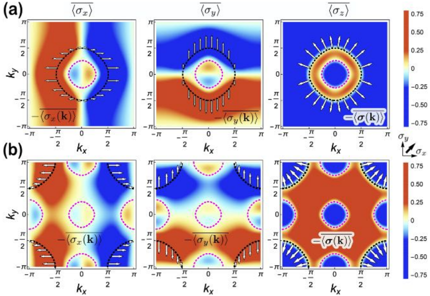

Figure 9: Numerical results for 2D topological phase with different quench protocal βt, with $m_x = m_y = 0$, $t_{so}^{x,y} = 0.6t_0$, and $\beta = 0.8$ by setting $t_0 = 1$. (a)Time-averaged spin textures are plotted after slow quench from $t = -10$ (trivial) to $t = 0$ (topological) with $m_z = t_0$. SIS is shown pink dashed ring with $\overline{\langle \boldsymbol{\sigma} \rangle} = 0$ while BIS is shown by black dashed ring. The white arrows denote the topological spin texture, composed of $-\overline{\langle \sigma_{x,y} \rangle}$, indicating Chern number $C_1 = -1$. (b) Same case with $m_z = -t_0$. Here the BIS are located at four corners of Brillouin Zone. From the white arrows, we identify the topological phase with the Chern number $C_1 = 1$ opposite to that in (a).

Slow Quench of Higher Dimensional Phases

Non-adiabatic Characterization of 3D Chiral Topological Phases

The Hamiltonian of 3D Topological Phases

$$H(\mathbf{k}) = \sum_{j=0}^{3} h_j(\mathbf{k})\gamma_j;$$

$$h_0 = \frac{g}{t} + m_z - t_0 \sum_i \cos k_i;$$

$$h_i = t_{so} \sin k_i, \text{ with } i = x, y, z;$$

Which,

$$\gamma_0 = \sigma_z \otimes \tau_x, \ \gamma_1 = \sigma_x \otimes 1,$$

$$\gamma_2 = \sigma_y \otimes 1, \ \gamma_3 = \sigma_z \otimes \tau_z;$$

For $t_0 < m_z < 3t_0$

$\Rightarrow \nu_3 = -1,$

For $-t_0 < m_z < t_0$

$\Rightarrow \nu_3 = 2,$

For $-3t_0 < m_z < -t_0$

$\Rightarrow C_1 = -1.$

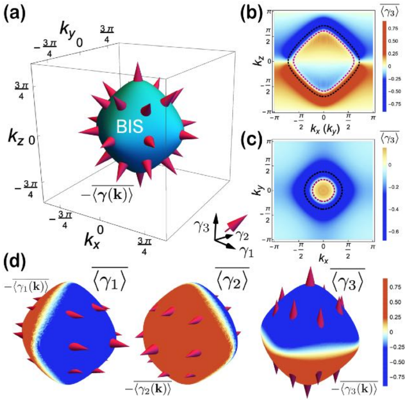

Figure 10: Non-adiabatic characterization of 3D case. The quench is simulated numerically from $t = 0.015$ to 1000, with $t_{so} = 0.2t_0$ and $g = 1$ by setting $t_0 = 1$. (a)The BIS (sphere) defined by $\overline{\langle\gamma_0(\boldsymbol{k})\rangle} = 0$ and the topological spin texture field $-\overline{\langle\boldsymbol{\gamma}(\boldsymbol{k})\rangle}$ (pink arrows), composed of the three components $-\overline{\langle\gamma_{1,2,3}(\boldsymbol{k})\rangle}$ [pink arrows on the three spheres in (d)]. (b) and (c) are $\overline{\langle\gamma_3\rangle}$ on cross sections $k_{x,y} = 0$ (b), and $k_z = \pi/2$ (c). (d) $\overline{\langle\gamma_{1,2,3}\rangle}$ on BIS. Their values of topological spin texture components are illustrated by pink arrows.

Section 6

Q & A

Any question about the "Minimal" scheme in detecting topological phases, provided by Non-adiabatic Quantum Dynamics ?

Any Question?
Supplement material

Theoretical derivation of $\hat{\vec{\sigma}}(t)$

$$\overline{\langle\vec{\sigma}(t)\rangle} = \lim_{T\to\infty}\frac{1}{T}\int_0^T dt\langle\psi_0|e^{iHt}\hat{\vec{\sigma}}e^{-iHt}|\psi_0\rangle;$$

$$\begin{aligned}\hat{\vec{\sigma}}(t) =& e^{iHt}\hat{\vec{\sigma}}e^{-iHt},\\ =&(\vec{n}\cdot\hat{\vec{\sigma}})\vec{n} + \cos 2\epsilon t[\hat{\vec{\sigma}} - (\vec{n}\cdot\hat{\vec{\sigma}})\vec{n}]\\ &- \sin 2\epsilon t(\hat{\vec{\sigma}}\times\vec{n});\end{aligned}$$

Which means

With the evolution of time, the Pauli vector revolves around the vector $\vec{h}$ with a cyclotron resonance motion of angular frequency $\omega = 2\epsilon$. The resonant motion may correspond to a physical image where electrons with spin magnetic moments do Larmor precession at an angular frequency of $\omega_{Lamor} = 2\epsilon$ in the

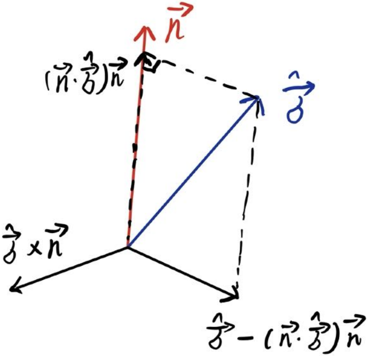

Figure 11: Vector $\hat{\vec{\sigma}}(t)$ precession sketch

Any Question?

Supplement material

Theoretical derivation of General Theoretical Model

$$
\begin{aligned}
H =& \vec{h} \cdot \hat{\vec{\sigma}} \\
=& \epsilon(\sin\theta\cos\phi, \sin\theta\sin\phi, \cos\theta) \cdot \hat{\vec{\sigma}} \\
=& \epsilon \begin{pmatrix} \cos\theta & \sin\theta e^{-i\phi} \\ \sin\theta e^{i\phi} & -\cos\theta \end{pmatrix};
\end{aligned}
$$

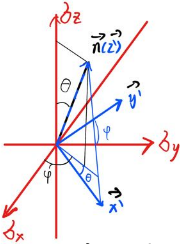

Figure 12: Rotation of coordinate sketch

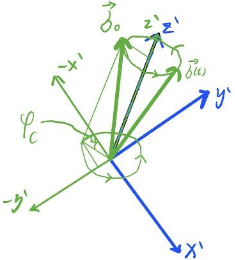

Figure 13: Vector $\hat{\vec{\sigma}}(t)$ precession in new coordinate sketch

$$
\begin{aligned}
\langle \vec{\sigma}(t) \rangle =& \langle \psi(t) | \hat{\vec{\sigma}} | \psi(t) \rangle \\
=& (|C_1|^2 - |C_2|^2)\vec{z'} \\
& - 2|C_1 C_2| \cos(2\epsilon t + \phi_c)\vec{x'} \\
& - 2|C_1 C_2| \sin(2\epsilon t + \phi_c)\vec{y'};
\end{aligned}
$$

$$
\overline{\langle \vec{\sigma}(t) \rangle} = (|C_1|^2 - |C_2|^2)\vec{n};
$$

In the Case of Sudden Quench

$$\overline{\langle\vec{\sigma}(t)\rangle} = (|C_1|^2 - |C_2|^2)\vec{n} = [-\cos(\theta-\theta_0) - \sin\theta\sin\theta_0(\cos(\phi-\phi_0)-1)]\vec{n}$$

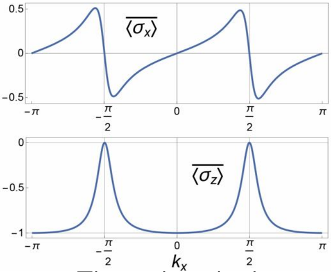

Figure 14: The analytical solution of 1D time average spin polarization $\overline{\langle\sigma_{x,y}\rangle}$

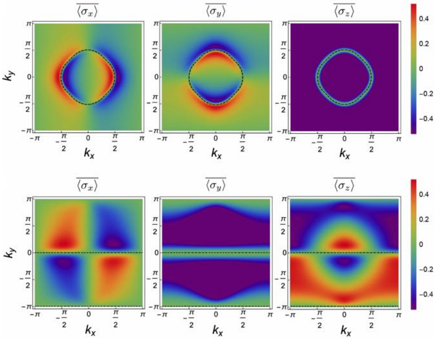

Figure 15: After different quenching processes, The analytical solution of 2D time average spin polarization $\overline{\langle\sigma_{x,y,z}\rangle}$

Universal drive model in Slow Quench

$$H(\vec{k}) = \begin{pmatrix} g/t + \epsilon(\vec{k})\cos[\theta(\vec{k})] & \epsilon(\vec{k})\sin[\theta(\vec{k})]e^{-i\phi(\vec{k})} \\ \epsilon(\vec{k})\sin[\theta(\vec{k})]e^{i\phi(\vec{k})} & -g/t - \epsilon(\vec{k})\cos[\theta(\vec{k})] \end{pmatrix}$$

$g \in [0, \infty)$ in the time-dependent Hamiltonian represents the quenching speed. The larger the g factor, the slower the quenching rate. When $g = 0$, the model degenerates into the Sudden Qunch model.

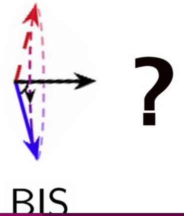

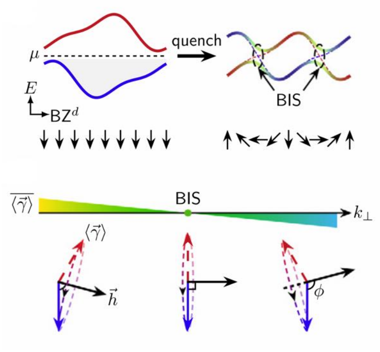

Figure 16: After a Sudden Quench, the spin precession near the BIS

Dynamic characterization in Slow Quench

$$\overline{\langle\vec{\sigma}(t)\rangle} = (|P_+|^2 - |P_-|^2)\vec{n} = \frac{2e^{-2\pi g}\cos[\theta(\vec{k})] - e^{-2\pi g} - e^{2\pi g}}{e^{2\pi g} - e^{-2\pi g}}\vec{n};$$

In BIS

$$\overline{\langle\sigma_i(k)\rangle} \neq 0, \quad \text{for } k \in BISs;$$

$$\overline{\langle\sigma_0(k)\rangle} = 0, \quad \text{for } k \in BISs;$$

In SIS

$$\overline{\langle\sigma_i(k)\rangle} = 0, \quad \text{for } k \in SISs, \; i = 0, 1, 2, \ldots, d$$

Dynamic characterization in Sudden Quench

$$\overline{\langle\vec{\sigma}(t)\rangle} = (|C_1|^2 - |C_2|^2)\vec{n} = [-\cos(\theta - \theta_0)$$

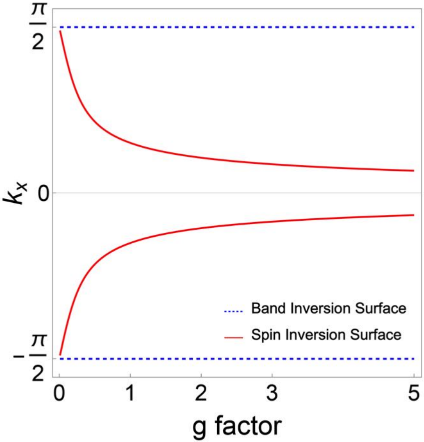

Figure 17: In 1D, Band Inversion Surface and Spin Inversion Surface change with the g factor.

Any Question?

Supplement material

Method for calculating Topological Number in 1D Slow Quench

$$v_1 \equiv \frac{1}{4\pi i}\int_{BZ} Tr[\gamma H(dH)]$$
$$= \ldots = \frac{1}{2}\sum_{BIS_j}[sgn(h_1, R_j) - sgn(h_1, L_j)];$$

In BIS

$$(|P_+|^2 - |P_-|^2)_{Slow}(\vec{k}) < 0;$$
$$sgn(h_1, R_j) = -sgn(\overline{\langle\sigma_x\rangle}, R_j)$$
$$sgn(h_1, L_j) = -sgn(\overline{\langle\sigma_x\rangle}, L_j);$$

$$v_1 = \frac{1}{2}\sum_{BIS_j}[sgn(\overline{\langle\sigma_x\rangle}, L_j) - sgn(\overline{\langle\sigma_x\rangle}, R_j)];$$

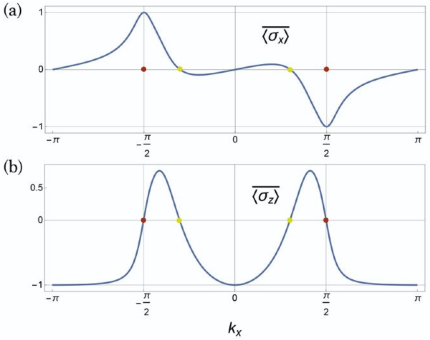

Figure 18: An example of a 1D slow Quench drive model. Red points represent BIS; Yellow points represent SIS;

Method for calculating Topological Number in 2D Slow Quench

$$Ch_1 = \frac{1}{4}\sum_{j,l} sgn(\overline{\langle\sigma_y\rangle}, j, l)\cdot sgnflip(\overline{\langle\sigma_x\rangle}, QB_{j,l}) - sgn(\overline{\langle\sigma_x\rangle}, j, l)\cdot sgnflip(\overline{\langle\sigma_y\rangle}, QB_{j,l});$$

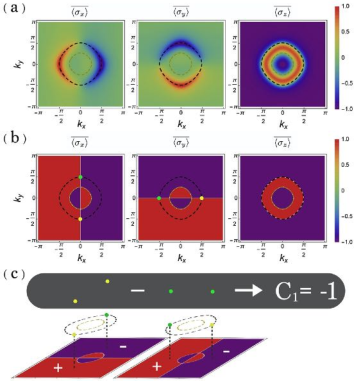

Figure 19: Slowly change m_z to $0 < m_z < 2t_0$ for slow quench drive

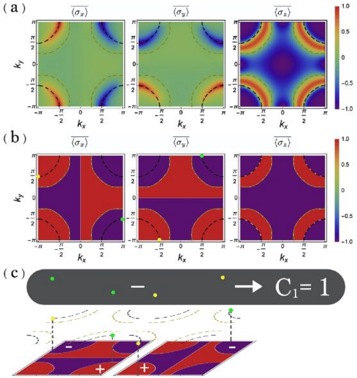

Figure 20: Slowly change m_z to $-2t_0 < m_z < 0$ for slow quench drive

Any Question?

Supplement material

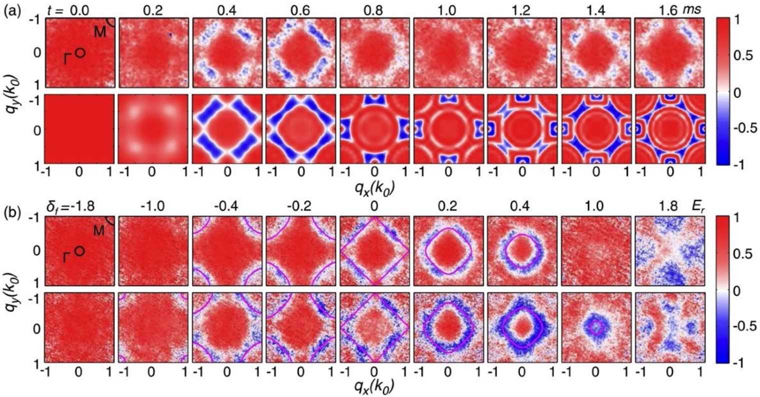

Figure 21: Ring structure of spin polarization in Experiment Data. (a) Evolution of $p(q, t)$ in the FBZ from $t = 0$ to 1.6 ms, with parameters $(V_0, \Omega_0) = (4.0, 1.0)E_r$ and $\delta_f = 0$. The upper row is from experimental measurements, and the lower row is from theoretical calculations. (b) Spin polarization in the FBZ at fixed evolution time t versus σ_f . The upper row is for $(V_0, \Omega_0) = (4.0, 1.0)E_r$ and t $t = 480\mu s$, and the lower row is for $(V_0, \Omega_0) = (4.0, 2.0)E_r$ and $t = 320\mu s$.

Sun W, Yi C-R, Wang B-Z, etc. Physical Review Letters, 2018, 121(25): 250403.

Emergent topology under slow non-adiabatic quantum dynamics

Junchen Ye
&
Fuxiang Li, Prof.

School of Physics and Electronics, Hunan University

Changsha 410082, China

July 26, 2020